Journal of Dental Sciences 19 (2024) 1801–1810

Available online at www.sciencedirect.com

ScienceDirect

journal homepage: www.e-jds.com

Original Article

Procyanidin B2 enhances anti-inflammatory responses of periodontal ligament cells by inhibiting the dominant negative pro-inflammatory isoforms of peroxisome proliferator-activated receptor γ

Tadahiro Yamamoto [a†], Hang Yuan [a†], Shigeki Suzuki [a*], Eiji Nemoto [a], Masahiro Saito [b], Satoru Yamada [a]

[a] *Department of Periodontology and Endodontology, Tohoku University Graduate School of Dentistry, Sendai, Japan*
[b] *Department of Restorative Dentistry, Tohoku University Graduate School of Dentistry, Sendai, Japan*

Received 17 September 2023; Final revision received 23 September 2023
Available online 6 October 2023

KEYWORDS
Periodontitis;
IL-6;
Periodontal ligament;
Mouse experimental periodontitis model

Abstract *Background/purpose:* Periodontal breakdown in periodontitis is exacerbated by pro-inflammatory responses of periodontal stromal cells such as periodontal ligament fibroblasts (PDLFs). Procyanidin B2 (PB2) is a ligand of the peroxisome proliferator-activated receptor (PPARγ). Herein, we investigated the expression of PPARγ isoforms in PDLFs and periodontal tissue, and examined the effects of PB2 on PPARγ isoform-dependent antiinflammatory responses.
Materials and methods: PPARγ isoforms were examined by PCR. PPARγ isoform-dependent inflammatory functions and anti-inflammatory effects of PB2 in PDLFs were evaluated based on IL-6 expression. Co-immunoprecipitation analysis of fixed chromatin-tethered protein (CoIPfctp) was conducted to investigate the association of each PPARγ isoform with the NF-κB-transcriptional complex. The effects of PB2 on periodontitis progression were evaluated using a ligature-induced murine periodontitis model.
Results: Three isoforms of PPARγ were expressed in PDLFs and periodontal tissues, consisting of the main full-length isoform (PPARγ) and two dominant negative isoforms that lack the ligand binding domain, namely the ubiquitously-expressed isoform (PPARγ-UBI) and unknown isoform (PPARγ-PDL). PPARγ and PPARγ-UBI were predominantly expressed. CoIP-fctp revealed that PPARγ-UBI was selectively associated with NF-κB p65, a key transcriptional factor

* Corresponding author. Department of Periodontology and Endodontology, Tohoku University Graduate School of Dentistry, 4-1, Seiryo-machi, Aoba-ku, Sendai, 980-8575, Japan.
E-mail address: shigeki.suzuki.b1@tohoku.ac.jp (S. Suzuki).
† Tadahiro Yamamoto and Hang Yuan are equal contributors to this work and are designated as co-first authors.

https://doi.org/10.1016/j.jds.2023.09.027
1991-7902/© 2023 Association for Dental Sciences of the Republic of China. Publishing services by Elsevier B.V. This is an open access article under the CC BY-NC-ND license (http://creativecommons.org/licenses/by-nc-nd/4.0/).

of IL-6 expression. PB2 suppressed LPS-induced-IL-6 expression exacerbated by the overexpression of PPARγ-UBI. In the murine periodontitis model, topical application of PB2 significantly mitigated alveolar bone loss.
Conclusion: These results suggest that the anti-inflammatory effects of PB2 in periodontal tissues/cells are distinct, and these effects arise from the inhibition of PPARγ-UBI; hence, the application of PB2 and modification of the splicing event in three PPARγ isoforms have therapeutic potential for preventing periodontitis.
© 2023 Association for Dental Sciences of the Republic of China. Publishing services by Elsevier B.V. This is an open access article under the CC BY-NC-ND license (http://creativecommons.org/licenses/by-nc-nd/4.0/).

Introduction

Periodontitis accompanied by alveolar bone loss and the irreversible breakdown of periodontal epithelial and connective attachment is developed by a local pathogenic bacterial infection that induces the production of cytokines and enzymes from host cells as a result of the host's protective inflammatory response.[1] The excess amount of pro-inflammatory cytokines, such as IL-6, TNF-α, and IL-1β, in inflamed periodontal tissue that is mainly secreted from infiltrated immunological cells, such as macrophages, neutrophils, and T cells, play a major role in the onset and progression of periodontitis.[1] Periodontal stromal cells, such as periodontal ligament fibroblasts (PDLF), osteoblasts/osteocytes, and gingival fibroblasts, also participate in the onset and progression of periodontal diseases by secreting pro-inflammatory cytokines, circulating RNAs, and RANKL, which is a ligand for the RANK receptor of the osteoclast precursor.[2,3] Moreover, IL-6 secreted from PDLF influences periodontal tissue breakdown.[4] NF-κB, an inflammatory signal, is active and required for expressing pro-inflammatory cytokines in the stromal cells, similar to immunological cells.[5,6] The importance of the NF-κB signal in periodontal stromal cells for periodontal tissue breakdown has been revealed by examining osteoblasts/osteocyte-specific inactivation of NF-κB eliminated alveolar bone loss in an experimental periodontitis mouse model.[7] Thus, protection of aberrant NF-κB activation in periodontal stromal cells is considered to be key for preventing periodontitis.

Peroxisome proliferator-activated receptor (PPARγ) is a nuclear receptor that plays a role in energy metabolism and osteogenic/cementogenic differentiation of PDLF.[8,9] In addition, PPARγ aids in inhibiting excess inflammation in both the acute and chronic stages. PPARγ suppresses the expression of a subset of Toll-like receptors (TLR),[10] and ligand-activated PPARγ directly associates with NF-κB to inhibit its transcriptional abilities.[11] Furthermore, rosiglitazone, an exogenous agonist of PPARγ that belongs to the family of thiazolidinedione compounds (TZD), was systemically injected into periodontal tissue of a ligature-induced rat periodontitis model and prevented alveolar bone loss, presumably by inhibiting osteoclastogenesis.[12] TZDs were previously administered to patients with type II diabetes as

Table 1 Primer pairs used in this study.

Primer name	Species	Direction	Sequence
PPARG	Human	forward	GAGCCCAAGTTTGAGTTTGC
		reverse	GGCGGTCTCCACTGAGAATA
PPARG-UBI	Human	forward	AATCAACCGCCCAGGTTT
		reverse	CTGTGAGGACTCAGGGTGGT
PPARG-PDL	Human	forward	TGCAGTGGGGATGTCTCATA
		reverse	CTGCAGTAGCTGCACGTGTT
IL-6	Human	forward	AAGCCAGAGCTGTGCAGATG
		reverse	GTTGGGTCAGGGGTGGTTAT
MCP-1	Human	forward	AGCAAGTGTCCCAAAGAAGC
		reverse	GAGTTTGGUTTTGCTTGTCC
COL1A1	Human	forward	GTGCTAAAGGTGCCAATGGT
		reverse	ACCAGGTTCACCGCTGTTAC
OCN	Human	forward	GGCGCTACCTGTATCAATGG
		reverse	TCAGCCAACTCGTCACAGTC
HPRT	Human	forward	TGGCGTCGTGATTAGTGATG
		reverse	CGAGCAAGACGTTCAGTCCT

PPARG = full-length PPARG, *PPARG-UBI* = PPARG ubiquitous isoform, *PPARG-PDL* = PPARG PDL specific isoform, *IL-6* = Interleukin-6, *MCP-1* =Monocyte chemoattractant protein-I, *COL1A1* = Collagen type I alpha 1 chain, *OCN* = Osteocalcin, *HPRT* = Hypoxanthine Phosphoribosyltransferase 1.

the first choice drug to improve insulin resistance; however, TZDs have recently become less prevalent due to the potential carcinogenicity.[13] Long-chain fatty acids, 15-deoxy-Δ12,14-PGJ2, oxidized LDL, and their metabolites are endogenous agonists of PPARγ,[14] but their specificity as PPARγ ligands has not been fully validated. Procyanidin B2 (PB2), a member of the flavonoids, has recently been identified as a PPARγ ligand and showed favorable systemic effects for reducing the risks of cardiovascular diseases, type II diabetes, and cancers.[15,16] Dietary flavonoids and

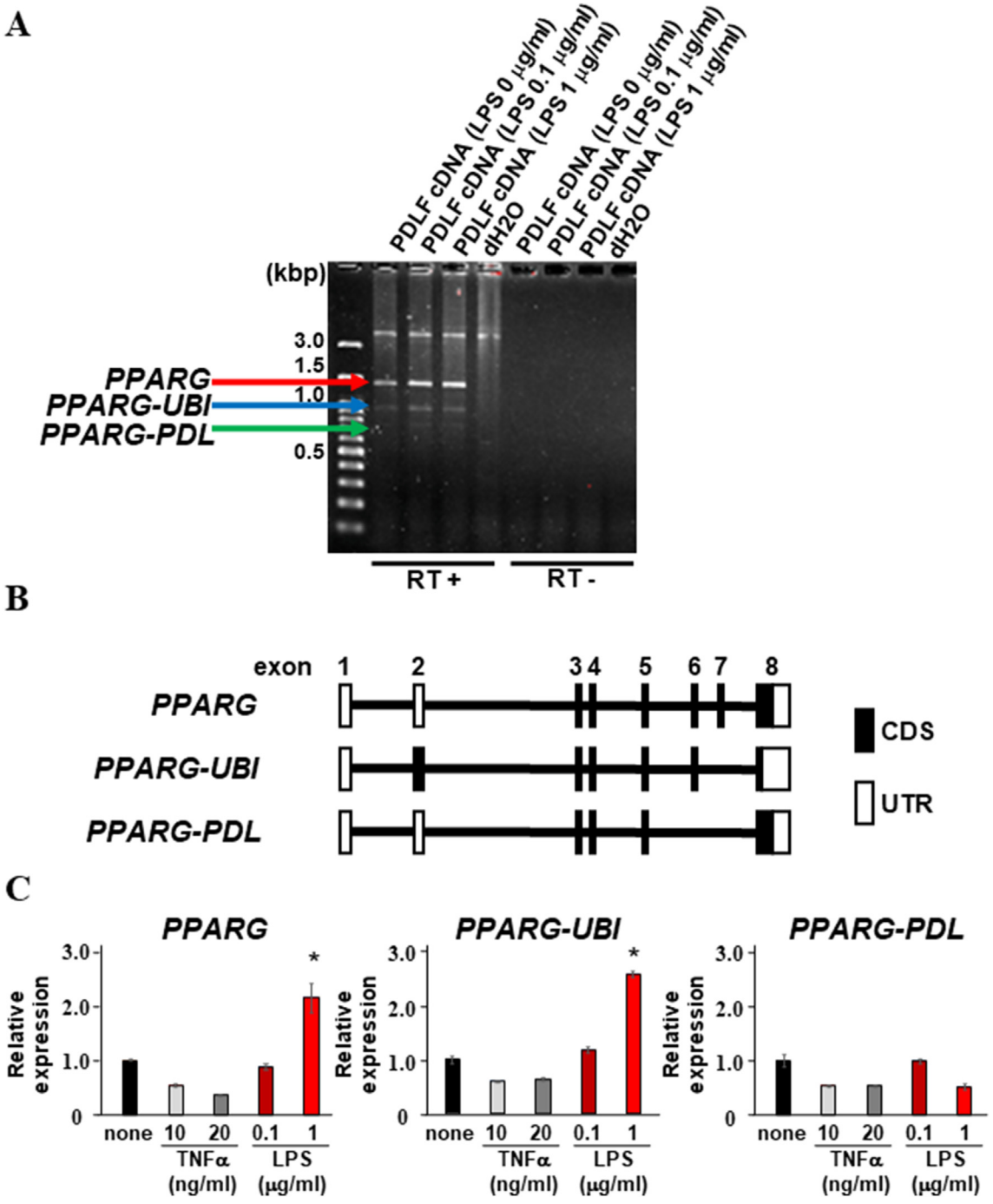

Figure 1 PPARγ isoforms identification in PDLFs. (A) PDLFs were stimulated with LPS for 24 h and then total RNA was collected. PPARG isoform expression was evaluated using the primer pairs amplifying from exon 2 to 8 for full-length *PPARG*. (B) Schematic view of three PPARG isoforms identified in PDLFs. (C) PDLFs were stimulated with TNF-α or LPS for 24 h and then total RNA was collected to analyze the expression changes of *PPARG*, *PPARG-UBI*, and *PPARG-PDL*. Each column represents the mean ± SD, where n = 3 for each group. *P < 0.05, significantly higher than non-treated. cDNA = complementary DNA, LPS = lipopolysaccharide, Kbp = kilo base pair, RT = reverse transcriptase, CDS = coding sequence, ORF = open reading frame.

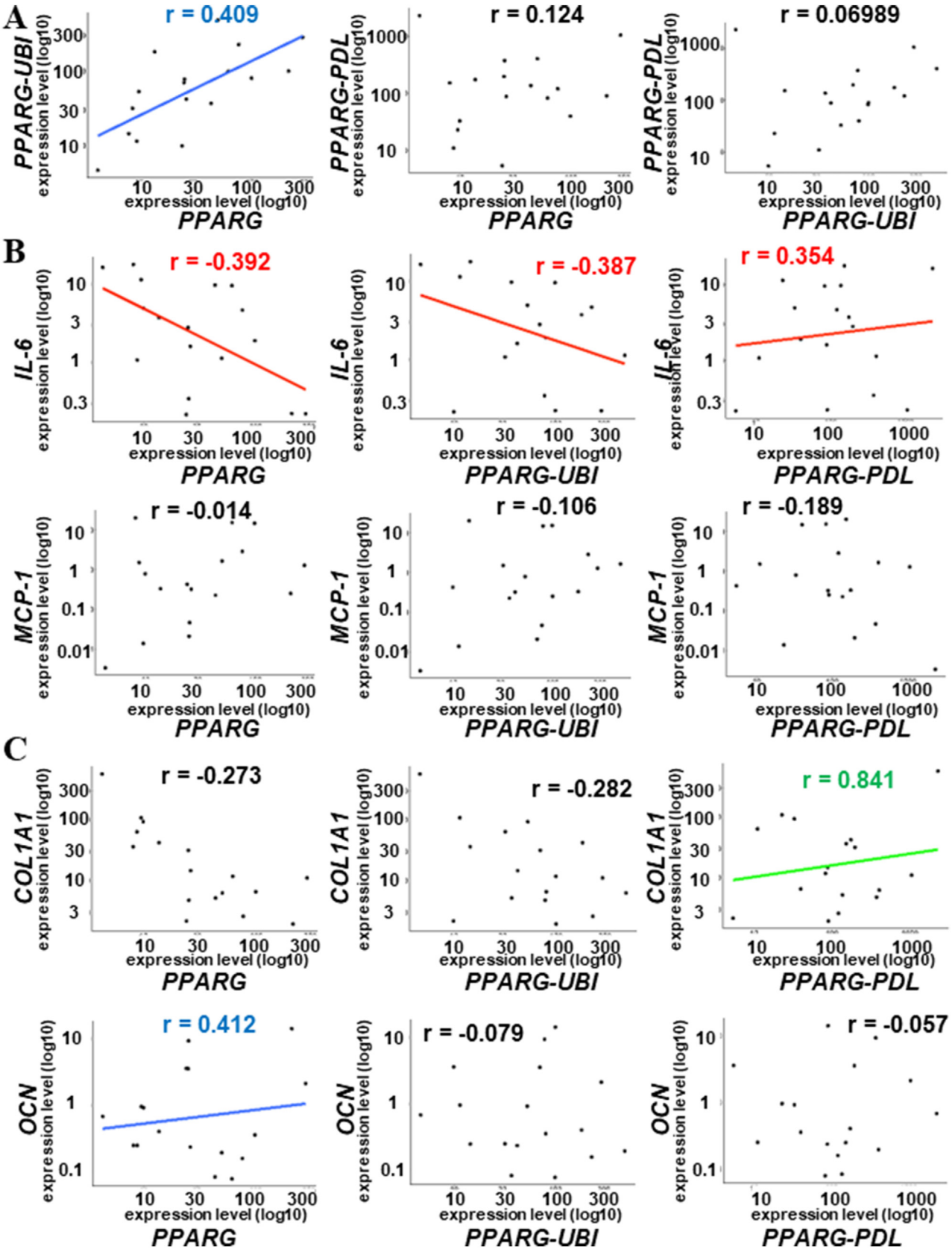

Figure 2 PPARγ isoforms identification in human clinical periodontal tissue. Inflamed clinical periodontal tissues (18 samples from different patients) were collected, and the expression levels of three *PPARG* isoforms, *MCP-1*, *COL1A1*, *IL-6*, and *OCN* were compared. High correlation ($r > 0.8$ or $r < -0.8$), moderate correlation ($0.4 < r < 0.8$ or $-0.8 < r < -0.4$), and weak correlation

isoflavonoids, such as epigallocatechin-3-gallate and quercetin, inhibit excess inflammation in periodontal tissue and cells.[17–19]

Moreover, various splicing isoforms of PPARγ have been detected.[20–23] The dominant negative isoform identified in adipocytes possesses a DNA binding domain but lacks the ligand binding domain, and therefore, competitively prevents full-length PPARγ association with co-transcriptional factor RXR, and the relative expression level of dominant negative *PPARG* was directly correlated with the body mass index in clinical samples.[23] Thus, isoform-dependent functions have been disclosed; however, the types and functions of *PPARG* isoforms in PDLFs and isoform-specific abilities for binding to NF-κB and modulating the effects of NF-κB remain unclarified.

In the present study, 3 isoforms of PPARγ in PDLFs and clinical periodontal tissue were identified, and their relations to *IL-6* expression were revealed. Then, the effects of PB2 on periodontitis onset and progression were clarified to reveal the isoform-specific favorable effects for inflammatory responses of PDLFs.

Materials and methods

Clinical sample preparation

This study was approved by the Ethics Committee of the Tohoku University Graduate School of Dentistry (approval number: 2020-3-045). Written informed consent was obtained from the patients. Inflamed periodontal tissues removed during non-surgical and surgical periodontal treatments were collected, immersed in RNAiso plus (Takara Bio Inc., Otsu, Japan) and sonicated with a homogenizer (Tomy, Tokyo, Japan).

Reagents

Procyanidin B2 (19865) was purchased from Cayman Chemical (Ann Arbor, MI, USA). LPS (127–05141) was purchased from Fujifilm Wako Pure Chemical Corporation, Ltd. (Osaka, Japan).

Isoforms identification

Entire mRNA sequence identification was conducted as described previously.[24] *PPARG* isoforms were amplified from the human PDLF cDNA sample using KOD DNA Polymerase (Toyobo Life Science, Tokyo, Japan) with a forward primer (AAGGCCATTTTCTCAAACGA) associating exon 2 and a reverse primer (CTGCAGTAGCTGCACGTGTT) associating exon 8 of full-length PPARG (ENST00000397010.7 PPARG-205).

Cell culture and stable cell generation

Human PDLFs were purchased from Lonza Inc. (Walkersville, MD, USA) and maintained in low glucose Dulbecco's Modified Eagle Medium (DMEM; Thermo Fisher Scientific, Carlsbad, CA, USA) supplemented with 100 units/ml of penicillin, 100 μg/ml of streptomycin, and 10% fetal bovine system. PDLFs were cultivated at 37 °C under humidified atmospheric conditions (5% CO_2 and 95% air). For generating PDLFs stably expressing the full-length (PPARγ), ubiquitous (PPARγ-UBI), and periodontal isoforms of PPARG (PPARγ-PDL), PPARγ, PPARγ-UBI, and PPARγ-PDL, sequences were amplified from the human PDLF cDNA generated using SSIV (Thermo Fisher Scientific) with reverse primers that had the FLAG coding sequence. These procedures were previously described in detail.[25]

Quantitative PCR (qPCR) analysis

Total RNA purification, cDNA preparation, and qPCR reactions were conducted as described previously.[26,27] Human *HPRT* was used as an internal reference control. PCR primer sequences for target genes are shown in Table 1.

Immunoblotting

Immunodetection was conducted as described previously.[28] Briefly, reduced samples were loaded onto NuPAGE Bis-Tris (Thermo Fisher Scientific) gels in MOPS buffer, and separated proteins were transferred onto a polyvinylidene fluoride membrane for immunodetection using the anti-FLAG (66008-4, 1:1000, Proteintech, Rosemont, IL, USA) and anti-p65 (Cell Signaling Technology, D14E12) antibodies as the primary antibodies.

Co-immunoprecipitation analysis of fixed chromatin-tethered protein (CoIP-fctp)

Sub-confluent PDL transfectants were pre-incubated with 4 μM of MG132, a proteasome inhibitor, for 6 h and fixed with 1.5% formaldehyde for 10 min. Cells were washed twice with Dulbecco's phosphate-buffered saline (DPBS) and then scraped off. Cell pellets were dissolved in ChIP sonication cell lysis buffer (Cell Signaling Technology, component of #81804) and incubated for 10 min at 4 °C. After centrifugation, cell pellets were mixed with ChIP sonication nuclear buffer (Cell Signaling Technology, component of #81804) and sonicated. The lysates were 10-fold diluted with DPBS and mixed with anti-p65 (Cell Signaling Technology, D14E12, 1:100). Tubes were rotated overnight at 4 °C. The next day, Protein G beads were added to each tube and mixed for 3 h at 4 °C. Then, the beads were washed and mixed with LDS sample buffer and reverse-crosslinked. The collected proteins were loaded onto SDS-PAGE as described previously.

Experimental animals

The study was carried out in compliance with the ARRIVE 2.0 guidelines. All experimental procedures conformed to the "Regulations for Animal Experiments and Related Activities at Tohoku University" and were reviewed by the Institutional Laboratory Animal Care and Use Committee of

($0.3 < r < 0.4$ or $-0.4 < r < -0.3$) are indicated by green, blue, and red lines, respectively. (For interpretation of the references to colour in this figure legend, the reader is referred to the Web version of this article.)

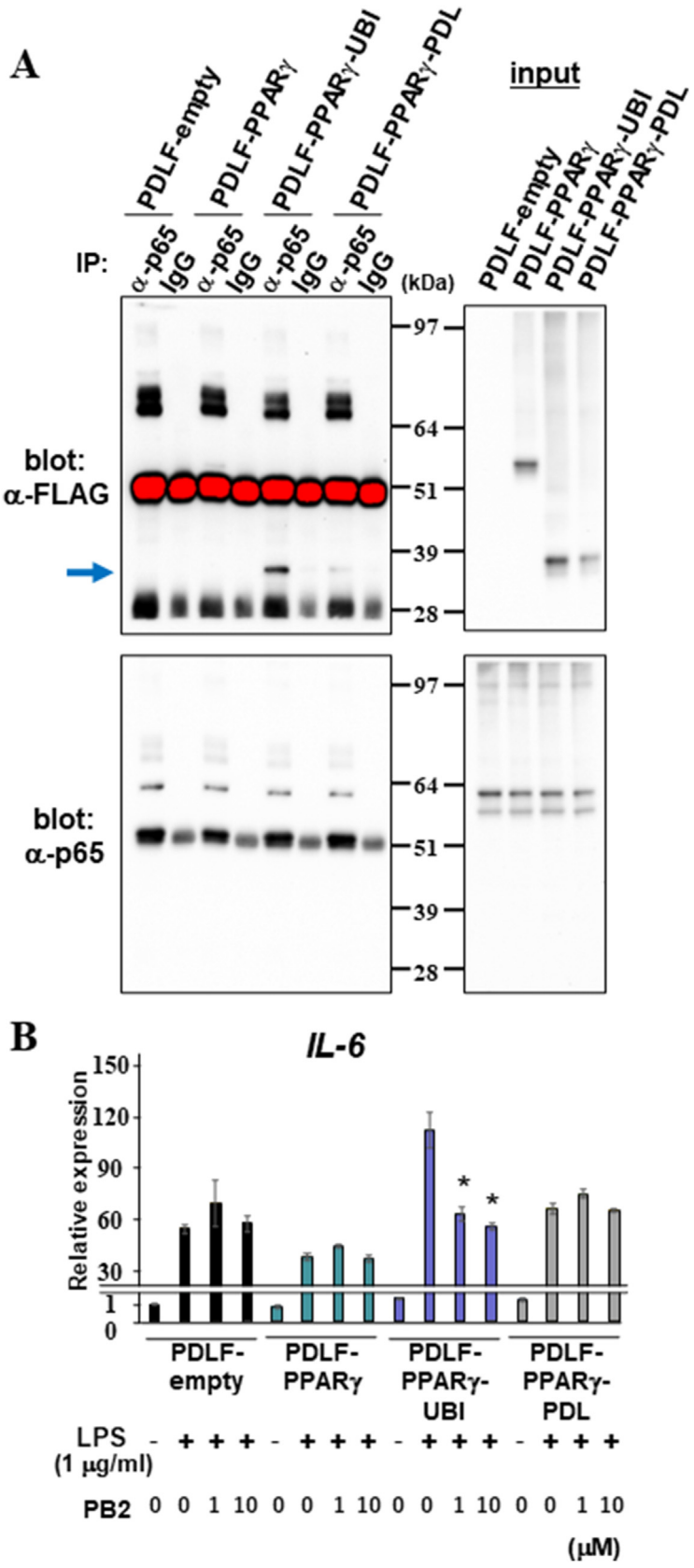

Figure 3 PDLF-PPARγ-UBI enhances IL-6 expression but PB2 restores it. (A) p65-immunoprecipitated and input samples of PDLF-empty, PDLF-PPARγ, PDLF-PPARγ-UBI, and PDLF-PPARγ-PDL were separately loaded onto SDS-PAGE, and the association of transgene products, namely PPARγ, PPARγ-UBI, and PPARγ-PDL, were analyzed by immunodetection of FLAG using the anti-FLAG antibody. Then, the membranes were stripped, and equivalent amounts of loaded proteins were confirmed using the anti-p65

Tohoku University, and finally, approved by the President of the University (Permit No. 2018DnA-043-08). Eleven-week-old male C57BL6/J mice (specific pathogen-free grade) were purchased from CLEA Japan, Inc. The mice were anesthetized, and silk ligatures (Elp Sterile Blade Silk, Black, 5–0, Akiyama Medical MFG. CO., LTD, Tokyo, Japan) were tied around their second maxillary molars for 14 days. For evaluating the effects of PB2 on periodontal tissue breakdown, PB2 dissolved in DPBS was topically administered (5, 10, or 20 mg/kg) every other day during the 14-day periodontal inflammation period. Mice in the control group were administered the same amount of DPBS in the same manner, with the same frequency.

Micro-computed tomography

Micro-computed tomography (μCT) was conducted as described previously.[29] The hemimaxillae were dissected, fixed for 24 h in 4% paraformaldehyde, and stored in DPBS at 4°C. Samples were scanned using a μCT scanner (Scanxmate-E090, Comscantecno Co. Ltd., Yokohama, Japan) with an isotropic resolution of 50 μm. All images were re-oriented, aligning the tomographic coronal plane of the second molar 2D images parallel to the buccal-lingual center line and coronal-apical center line. The vertical distances from the cementoenamel junction (CEJ) to the alveolar bone crest at the mesial and distal roots were measured and summed. This sum was used for quantitatively comparing bone regeneration levels in the periodontal regeneration stage.

Histology

The maxilla samples used for μCT analysis were decalcified with 0.134 mol of EDTA in DPBS at 4°C for 2 weeks. Masson's Trichrome staining was performed on 5 μm-thick paraffin sections, as described previously.[30] Histological images were captured using an upright microscope (DM6000 B: Leica, Wetzlar, Germany) with a digital camera (DP28: Olympus, Tokyo, Japan).

Statistical analysis

Statistical analysis was performed by one-way analysis of variance, followed by the Tukey test (Fig. 1) and two-tailed unpaired Student's t-test (Figs. 3 and 4).

Results

PPARγ isoform identification in PDL tissue and PDLFs

To determine which *PPARG* isoforms are present in PDLFs, PCR was conducted to detect *PPARG* transcribed products expanding from exon 2 to exon 8 of full-length *PPARG*, and ultimately, three *PPARG*-specific bands were identified (Fig. 1A). DNA sequencing of the amplified products revealed that the longest one was full-length *PPARG*, as expected, followed by the spliced isoform lacking exon 7 (ubiquitous isoform: *PPARG-UBI*), which was previously identified in tissues other than PDLFs or periodontal tissue.[23] The shortest isoform lacked exons 6 and 7 (PDL specific isoform: *PPARG-PDL*), which has not been previously reported according to Ensembl genome browser (access date 2023/08/29) (Fig. 1B). DNA sequencing of the band that migrated more than 1.5 kB revealed non-specific amplification (data not shown). Since none of the bands were observed in the samples without reverse transcriptase, these bands arose from transcripts and not potentially contaminated DNA. The expression of these three isoforms was decreased by TNF-α (Fig. 1C). The expression of *PPARG* and *PPARG-UBI* were significantly up-regulated by the treatment with LPS (1 μg/ml), but that of *PPARG-PDL* was suppressed.

Next, clinical periodontal tissue samples were obtained during surgical or non-surgical periodontal treatment to examine whether *PPARG*, *PPARG-UBI*, and *PPARG-PDL* are expressed in periodontal tissue *in vivo* and whether there is a correlation between the expression levels of the three isoforms (Fig. 2A). The direct correlation between *PPARG* and *PPARG-UBI* was identified ($r = 0.40868$), but no apparent correlation between *PPARG* and *PPARG-PDL* ($r = 0.12383$) or between *PPARG-UBI* and *PPARG-PDL* ($r = 0.06989$) was revealed. Then, *IL-6* expression was inversely correlated with *PPARG* ($r = -0.39216$) and *PPARG-UBI* ($r = -0.38720$) and directly correlated with *PPARG-PDL* ($r = 0.35362$), as shown in Fig. 2B. *MCP-1* expression was not correlated with *PPARG*, *PPARG-UBI*, or *PPARG-PDL*. For correlation with extracellular matrix-coding genes (Fig. 2C), *COL1A1* expression was only correlated with *PPARG-PDL* ($r = 0.84136$), and *OCN* expression was only correlated with *PPARG* ($r = 0.41187$).

PDLF-PPARγ-UBI induces *IL-6* expression and PB2 restores increased-*IL-6* expression in PDLF-PPARγ-UBI

The PDLFs over-expressing *PPARG* (PDLF-PPARγ-FLAG), *PPARγ-UBI* (PDLF-PPARγ-UBI-FLAG), or *PPARG-PDL* (PDLF-PPARγ-PDL-FLAG) were generated, and co-immunoprecipitation of chromatin-tethered protein assay (CoIP-ctps) was performed to examine the interaction between p65 and PPARγ, PPARγ-UBI, or PPARγ-PDL, revealing that only PPARγ-UBI localized in the vicinity of p65 (Fig. 3A, arrow). Next, to assess the anti-inflammatory abilities of these 4 transfectants, cells were stimulated with LPS (1 μg/ml) in the presence or absence of PB2 (1 and 10 μM) (Fig. 3B). LPS increased *IL-6* expression in all 4 types of PDLF transfectants. PB2 suppressed LPS-induced *IL-6* expression in PPARγ-UBI. In contrast, PB2 did not suppress

antibody. (B) PDLF-empty, PDLF-PPARγ, PDLF-PPARγ-UBI, and PDLF-PPARγ-PDL were stimulated with LPS in the presence or absence of PB2 (1 and 10 μM), and then total RNA was collected to quantify the expression of *IL-6*. *HPRT* was used for normalization. *$P < 0.05$, significantly lower than the transfectant treated with LPS alone. IP = immunoprecipitation, LPS = lipopolysaccharide, PB2 = Procyanidin B2.

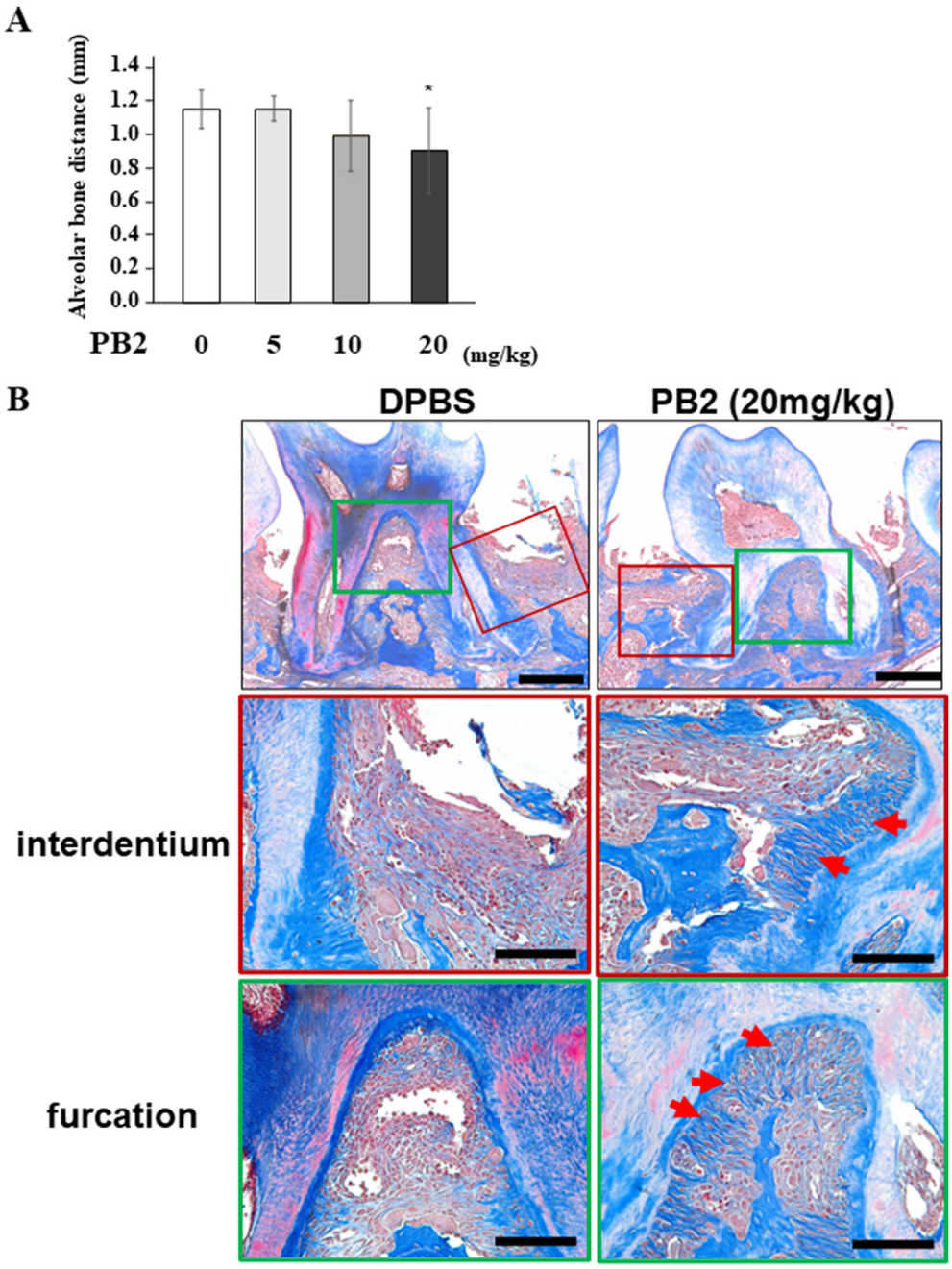

Figure 4 PB2 prevents periodontal tissue breakdown in ligature-induced experimental periodontitis. (A) The vertical distances from the CEJ to the alveolar bone crest at the mesial and distal roots on day 14 were measured and summed (n = 8). (B) Demineralized male maxilla sections of the mice treated with 0 or 20 mg/kg collected on day 14 were stained with Masson's trichrome. *P < 0.05, significantly different from the control. Scale bars correspond to 300 and 100 μm at low and high magnification, respectively. Red arrows indicate collagen fibers in PDL tissue. PB2 = Procyanidin B2. (For interpretation of the references to colour in this figure legend, the reader is referred to the Web version of this article.)

LPS-induced *IL-6* expression in PDLF-empty, PDLF-PPARγ, or PDLF-PPARγ-PDL.

PB2 prevents periodontal tissue breakdown in ligature-induced experimental periodontitis

To investigate whether PB2 possesses protective functions for periodontal tissue *in vivo*, ligature-induced periodontitis was induced for 14 days, and meanwhile, PB2 (5, 10, and 20 mg/kg) or DPBS was locally applied into the mesial and distal sides of the ligated upper second molar every other day. Quantitative analysis of the distance between the cementum-enamel junction and alveolar bone crest at day 14 showed that the distance was significantly narrow in the ligated teeth treated with PB2 compared with the ligated teeth treated with DPBS, indicating that PB2 administration reduced bone loss (Fig. 4A). The images for

Masson trichrome staining of ligated second molars at day 14 showed that PB2 treatment suppressed infiltration of immunological cells and conserved Sharpey's fiber structure in PDL tissue of furcation area and interdentium (red arrows) (Fig. 4B).

Discussion

The present study demonstrated that periodontal tissue/cells express three isoforms of PPARγ, namely full-length PPARγ and 2 dominant negative types, PPARγ-PBI and PPARγ-PDL (Figs. 1 and 2). PB2 suppressed PPARγ-PBI-induced *IL-6* expression in PDLFs, and PB2 topical application inhibited periodontal tissue breakdown in ligature-induced murine periodontitis.

PB2 has shown anti-inflammatory effects promoting M2 macrophage polarization.[14] PB2 also contributes to the attenuation of hepatocyte pyroptosis depending on PPARγ and requires Nrf2-induced PPARγ expression to ameliorate endothelial dysfunction in preeclampsia.[31,32] Thus, the favorable effects of the PB2-PPARγ axis are not limited to particular cell types. During prolonged periodontal chronic inflammation and following periodontal destruction stages, various types of immunological cells predominantly participate in pathogenesis with T cells and B cells in the early and late stages of periodontal progression, respectively.[33] Therefore, protective effects of PB2 for periodontal breakdown in the murine periodontitis model do not solely arise from inhibition of pro-cytokine secretion from stromal cells (Fig. 4). PB2 is obtained by ingesting apples, cherries, cocoa, and grape seeds, and has been reported to exhibit multiple beneficial functions in PPARγ-dependent and independent manners, such as antioxidative activity, mitigation of endoplasmic reticulum stress, and anti-inflammatory effects, without any negative effects, even a high dose.[32,34—36] Further studies are required to identify how PB2 topical injection ameliorates periodontal inflammation by focusing on the interaction between stromal mesenchymal cells, such as PDLFs, and infiltrated immunological cells such as macrophages.

Among the three PPARγ isoforms, PPARγ-PDL lacking exons 6 and 7 was newly identified in this study (Fig. 1). PPARγ-UBI lacking exon 7 was identified in adipose tissue, and SRSF1, a member of the serine/arginine-rich splicing factor, is required for expressing PPARγ and PPARγ-UBI.[23] Approximately 7000 monogenic hereditary diseases have been reported, one-third of which arise from splicing mutations.[37—39] Thus, similar to adipocytes, SRSFs possibly participate in the expression of PPARγ-UBI and PPARγ-PDL. Only PPARγ-UBI, not PPARγ or PPARγ-PDL, localized in the vicinity of the p65-associated chromatin region in PDLFs and suppressed LPS-induced *IL-6* expression (Fig. 3). Thus, PPARγ-UBI might guide transcriptional activators to the *IL-6* promoter region where p65 associates; however, further analyses are required to reveal the three-dimensional p65 binding structure in PPARγ-UBI, but not in PPARγ or PPARγ-PDL, elucidate the specificity of PPARγ-UBI and possible inhibition by PB2, and evaluate the extent to which favorable outcomes by PB2 rely on PPARγ-UBI inhibition. LPS usually induces *IL-6* expression, and the treatment of PDLFs with a high dose of LPS increased PPARγ and PPARγ-UBI expression *in vitro* (Fig. 1), although PPARγ and PPARγ-UBI expression was inversely associated with *IL-6* expression *in vivo*. This discrepancy may indicate that the anti-inflammatory ability of PPARγ, a dominant isoform, is sufficient to down-regulate *IL-6* expression during the minor chronic inflammation stage observed in most clinical cases.

In conclusion, for the first time, this study demonstrated that PB2 protects periodontal tissue breakdown *in vivo*, and PB2 specifically suppresses the pro-inflammatory ability of PPARγ-UBI *in vitro*. Thus, the application of PB2 and artificial modification of the splicing event in three PPARγ isoforms have therapeutic potential for preventing periodontitis.

Declaration of competing interest

The authors have no conflicts of interest relevant to this article.

Acknowledgments

The present study was financially supported by JSPS KAKENHI Grant Number 19K10104, 22H03266, and 22K19611 for Shigeki Suzuki and 20H03862 and 20K21668 for Satoru Yamada.

References

1. Usui M, Onizuka S, Sato T, Kokabu S, Ariyoshi W, Nakashima K. Mechanism of alveolar bone destruction in periodontitis-periodontal bacteria and inflammation. *Jpn Dent Sci Rev* 2021;57:201—8.
2. Nilsson B. Mechanisms involved in regulation of periodontal ligament cell production of pro-inflammatory cytokines: implications in periodontitis. *J Periodontal Res* 2021;56:249—55.
3. Suzuki S, Yamada S. Epigenetics in susceptibility, progression, and diagnosis of periodontitis. *Jpn Dent Sci Rev* 2022;58:183—92.
4. Tsukasaki M, Komatsu N, Nagashima K, et al. Host defense against oral microbiota by bone-damaging T cells. *Nat Commun* 2018;9:701.
5. Jimi E, Takakura N, Hiura F, Nakamura I, Hirata-Tsuchiya S. The role of NF-κB in physiological bone development and inflammatory bone diseases: is NF-κB inhibition "killing two birds with one stone". *Cells* 2019;8:1636.
6. Hirata-Tsuchiya S, Suzuki S, Okamoto K, et al. A small nuclear acidic protein (MTI-II, Zn2+-binding protein, parathymosin) attenuates TNF-α inhibition of BMP-induced osteogenesis by enhancing accessibility of the Smad4-NF-κB p65 complex to Smad binding element. *Mol Cell Biochem* 2020;469:133—42.
7. Pacios S, Xiao W, Mattos M, et al. Osteoblast lineage cells play an essential role in periodontal bone loss through activation of nuclear factor-kappa B. *Sci Rep* 2015;5:16694.
8. Chui PC, Guan HP, Lehrke M, Lazar MA. PPARgamma regulates adipocyte cholesterol metabolism via oxidized LDL receptor 1. *J Clin Invest* 2005;115:2244—56.
9. Yuan H, Suzuki S, Hirata-Tsuchiya S, et al. PPARγ-induced global H3K27 acetylation maintains osteo/cementogenic abilities of periodontal ligament fibroblasts. *Int J Mol Sci* 2021;22:8646.
10. Dana N, Vaseghi G, Javanmard SH. Activation of PPARγ inhibits TLR4 signal transduction pathway in melanoma cancer in vitro. *Adv Pharmaceut Bull* 2020;10:458—63.

11. Hou Y, Moreau F, Chadee K. PPARγ is an E3 ligase that induces the degradation of NFκB/p65. *Nat Commun* 2012;3:1300.
12. Hassumi MY, Silva-Filho VJ, Campos-Júnior JC, et al. PPAR-gamma agonist rosiglitazone prevents inflammatory periodontal bone loss by inhibiting osteoclastogenesis. *Int Immunopharm* 2009;9:1150—8.
13. Soccio RE, Chen ER, Lazar MA. Thiazolidinediones and the promise of insulin sensitization in type 2 diabetes. *Cell Metabol* 2014;20:573—91.
14. Umeno A, Sakashita M, Sugino S, et al. Comprehensive analysis of PPARγ agonist activities of stereo-, regio-, and enantioisomers of hydroxyoctadecadienoic acids. *Biosci Rep* 2020; 40:BSR20193767.
15. Tian Y, Yang C, Yao Q, et al. Procyanidin B2 activates PPARγ to induce M2 polarization in mouse macrophages. *Front Immunol* 2019;10:1895.
16. Chuang Chia-Chi. Potential mechanisms by which polyphenol-rich grapes prevent obesity-mediated inflammation and metabolic diseases. *Annu Rev Nutr* 2011;31:155—76.
17. Chao-Yen H, Min Yee N, Taichen L, et al. Quercetin ameliorates advanced glycation end product-induced wound healing impairment and inflammaging in human gingival fibroblasts, *J Dent Sci*, doi:10.1016/ j.jds.2023.04.014.
18. Fan Q, Xiao-Hong Z, Teng-Fei W, et al. Effects of epigallocatechin-3-gallate on oxidative stress, inflammation, and bone loss in a rat periodontitis model. *J Dent Sci* 2023;18: 1567—75.
19. Maryam V, Farnoosh A, Ali A, et al. Uses of soybean isoflavonoids in dentistry: a literature review. *J Dent Sci*, https: //doi.org/10.1016/j.jds.2021.11.020.
20. Strand DW, Jiang M, Murphy TA, et al. PPARγ isoforms differentially regulate metabolic networks to mediate mouse prostatic epithelial differentiation. *Cell Death Dis* 2012;3:e361.
21. Choi JY, Park S. Role of protein kinase A and class II phosphatidylinositol 3-kinase C2β in the downregulation of KCa3.1 channel synthesis and membrane surface expression by lysoglobotriaosylceramide. *Biochem Biophys Res Commun* 2016; 470:907—12.
22. Hu W, Jiang C, Kim M, et al. Isoform-specific functions of PPARγ in gene regulation and metabolism. *Genes Dev* 2022;36: 300—12.
23. Aprile M, Cataldi S, Ambrosio MR, et al. PPARγΔ5, a naturally occurring dominant-negative splice isoform, impairs PPARγ function and adipocyte differentiation. *Cell Rep* 2018;25: 1577—92.
24. Suzuki S, Hoshino H, Yoshida K, et al. Genome-wide identification of chromatin-enriched RNA reveals that unspliced dentin matrix protein-1 mRNA regulates cell proliferation in squamous cell carcinoma. *Biochem Biophys Res Commun* 2018; 495:2303—9.
25. Yuan H, Suzuki S, Terui H, et al. Loss of IκBζ drives dentin formation via altered H3K4me3 status. *J Dent Res* 2022;101: 951—61.
26. Suzuki S, Fukuda T, Nagayasu S, et al. Dental pulp cell-derived powerful inducer of TNF-α comprises PKR containing stress granule rich microvesicles. *Sci Rep* 2019;9:3825.
27. Yoshida K, Suzuki S, Kawada-Matsuo M, et al. Heparin-LL37 complexes are less cytotoxic for human dental pulp cells and have undiminished antimicrobial and LPS-neutralizing abilities. *Int Endod J* 2019;52:1327—43.
28. Suzuki S, Kobuke S, Haruyama N, Hoshino H, Kulkarni AB, Nishimura F. Adhesive and migratory effects of phosphophoryn are modulated by flanking peptides of the integrin binding motif. *PLoS One* 2014;9:e112490.
29. Sato A, Suzuki S, Yuan H, et al. Pharmacological activation of YAP/TAZ by targeting LATS1/2 enhances periodontal tissue regeneration in a murine model. *Int J Mol Sci* 2023;24:970.
30. Jaha H, Husein D, Ohyama Y, et al. N-terminal dentin sialoprotein fragment induces type I collagen production and upregulates dentinogenesis marker expression in osteoblasts. *Biochem Biophys Rep* 2016;6:190—6.
31. Liu J, Yao Q, Xie X, et al. Procyanidin B2 attenuates nicotine-induced hepatocyte pyroptosis through a PPARγ-dependent mechanism. *Nutrients* 2022;14:1756.
32. Liu L, Wang R, Xu R, Chu Y, Gu W. Procyanidin B2 ameliorates endothelial dysfunction and impaired angiogenesis via the Nrf2/PPARγ/sFlt-1 axis in preeclampsia. *Pharmacol Res* 2022; 177:106127.
33. Gonzales José R. T- and B-cell subsets in periodontitis. *Periodontol* 2000 2015;69:181—200.
34. Zhang WY, Liu HQ, Xie KQ, et al. Procyanidin dimer B2 [epicatechin-(4beta-8)-epicatechin] suppresses the expression of cyclooxygenase-2 in endotoxin-treated monocytic cells. *Biochem Biophys Res Commun* 2006;345:508—15.
35. Nie X, Tang W, Zhang Z, et al. Procyanidin B2 mitigates endothelial endoplasmic reticulum stress through a PPARδ-dependent mechanism. *Redox Biol* 2020;37:101728.
36. Su H, Li Y, Hu D, et al. Procyanidin B2 ameliorates free fatty acids-induced hepatic steatosis through regulating TFEB-mediated lysosomal pathway and redox state. *Free Radic Biol Med* 2018;126:269—86.
37. Manning KS, Cooper TA. The roles of RNA processing in translating genotype to phenotype. *Nat Rev Mol Cell Biol* 2017;18: 102—14.
38. Sperling R. *The Nuts and Bolts of the Endogenous Spliceosome*. Wiley Interdiscip Rev RNA, 2017:8.
39. Ajiro M, Awaya T, Kim YJ, et al. Therapeutic manipulation of IKBKAP mis-splicing with a small molecule to cure familial dysautonomia. *Nat Commun* 2021;12:4507.